

# Compensation of intra-channel nonlinear fibre impairments using simplified digital back-propagation algorithm

Danish Rafique,<sup>1,\*</sup> Marco Mussolin,<sup>2,4</sup> Marco Forzati,<sup>3</sup> Jonas Mårtensson,<sup>3</sup> Mohsan N. Chughtai,<sup>3</sup> and Andrew D. Ellis<sup>1</sup>

<sup>1</sup>Photonics Systems Group, Tyndall National Institute and Department of Electrical Engineering/Physics, University College Cork, Dyke Parade, Prospect Row, Cork, Ireland

<sup>2</sup>Department of Information Engineering, University of Padova, Italy

<sup>3</sup>Acreo Netlab, Electrum 236, SE 16440, Kista, Sweden

<sup>4</sup>[mussolin@dei.unipd.it](mailto:mussolin@dei.unipd.it)

\*[danish.rafique@tyndall.ie](mailto:danish.rafique@tyndall.ie)

**Abstract:** We investigate a digital back-propagation simplification method to enable computationally-efficient digital nonlinearity compensation for a coherently-detected 112 Gb/s polarization multiplexed quadrature phase shifted keying transmission over a 1,600 km link (20x80km) with no inline compensation. Through numerical simulation, we report up to 80% reduction in required back-propagation steps to perform nonlinear compensation, in comparison to the standard back-propagation algorithm. This method takes into account the correlation between adjacent symbols at a given instant using a weighted-average approach, and optimization of the position of nonlinear compensator stage to enable practical digital back-propagation.

©2011 Optical Society of America

**OCIS codes:** (060.2330) Fiber optics communications; (060.1660) Coherent communications; (190.4370) Nonlinear optics, fibers.

## References and links

1. A. D. Ellis, J. Zhao, and D. Cotter, "Approaching the non-linear shannon limit," *J. Lightwave Technol.* **28**(4), 423–433 (2010).
2. M. Nakazawa, S. Okamoto, T. Omiya, K. Kasai, and M. Yoshida, "256 QAM (64 Gbit/s) coherent optical transmission over 160 km with an optical bandwidth of 5.4 GHz," *Optical Fiber Communication Conference'10, OThD5*, (2010).
3. G. Gavioli, E. Torrenzo, G. Bosco, A. Carena, V. Curri, V. Miot, P. Poggiolini, M. Belmonte, A. Guglielame, A. Brinciotti, A. La Porta, F. Forghieri, C. Muzio, G. Osnao, S. Piciaccia, C. Lezzi, L. Molle, and R. Freund, "100Gb/s WDM NRZ-PM-QPSK long-haul transmission experiment over installed fiber probing non-linear reach with and without DCUs," *European Conference on Optical Communications ECOC'09*, 3.4.2, (2009).
4. P. Serena, N. Rossi, and A. Bononi, "Nonlinear penalty reduction induced by PMD in 112 Gbit/s WDM PDM-QPSK coherent systems," *European Conference on Optical Communications ECOC'09*, 10.4.3, (2009).
5. C. S. Fludger, T. Duthel, D. van den Borne, C. Schulien, E.-D. Schmidt, T. Wuth, J. Geyer, E. De Man, Khoe Giok-Djan, and H. de Waardt, "Coherent equalization and POLMUX-RZ-DQPSK for robust 100-GE transmission," *J. Lightwave Technol.* **26**(1), 64–72 (2008).
6. M. Kuschnerov, F. N. Hauske, K. Piyawanno, B. Spinnler, M. S. Alfiad, A. Napoli, and B. Lankl, "DSP for coherent single-carrier receivers," *J. Lightwave Technol.* **27**(16), 3614–3622 (2009).
7. S. L. Jansen, D. van den Borne, B. Spinnler, S. Calabrò, H. Suche, P. M. Krummrich, W. Sohler, G.-D. Khoe, and H. de Waardt, "Optical phase conjugation for ultra long-haul phase-shift-keyed transmission," *J. Lightwave Technol.* **24**(1), 54–64 (2006).
8. E. Ip, "Nonlinear compensation using backpropagation for polarization-multiplexed transmission," *J. Lightwave Technol.* **28**(6), 939–951 (2010).
9. X. Li, X. Chen, G. Goldfarb, E. Mateo, I. Kim, F. Yaman, and G. Li, "Electronic post-compensation of WDM transmission impairments using coherent detection and digital signal processing," *Opt. Express* **16**(2), 880–888 (2008).
10. D. Rafique, J. Zhao, A.D. Ellis "Impact of dispersion map management on the performance of back-propagation for nonlinear WDM transmissions," *OECC*, 00107, (2010).
11. S. Oda, T. Tanimura, T. Hoshida, C. Ohshima, H. Nakashima, T. Zhenning, and J. C. Rasmussen, "112 Gb/s DP-QPSK transmission using a novel nonlinear compensator in digital coherent receiver," *Optical Fiber Communication Conference'09, OThR6*, (2009).

12. L. B. Du and A. J. Lowery, "Improved single channel backpropagation for intra-channel fiber nonlinearity compensation in long-haul optical communication systems," *Opt. Express* **18**(16), 17075–17088 (2010).
  13. X. Chongjin and R. J. Essiambre, "Electronic nonlinearity compensation in 112-Gb/s PDM-QPSK optical coherent transmission systems," *European Conference on Optical Communications ECOC'10, Mo.1.C.1*, (2010).
  14. M. Mussolin, M. Forzati, J. Martensson, A. Carena, and G. Bosco, "DSP-based compensation of non-linear impairments in 100 Gb/s PolMux QPSK," in *Transparent Optical Networks (ICTON)'10, We.D1.2* (2010).
  15. T. Tanimura, T. Hoshida, T. Tanaka, L. Lei, S. Oda, H. Nakashima, T. Zhenning, and J. C. Rasmussen, "Semi-blind nonlinear equalization in coherent multi-span transmission system with inhomogeneous span parameters," *Optical Fiber Communication Conference'09, OMR6*, (2010).
  16. G. P. Agrawal, *Nonlinear Fiber Optics* (Academic Press, 2007).
  17. S. J. Savory, G. Gavioli, R. I. Killey, and P. Bayvel, "Electronic compensation of chromatic dispersion using a digital coherent receiver," *Opt. Express* **15**(5), 2120–2126 (2007).
  18. D. Marcuse, C. R. Manyuk, and P. K. A. Wai, "Application of the Manakov-PMD equation to studies of signal propagation in optical fibers with randomly varying birefringence," *J. Lightwave Technol.* **15**(9), 1735–1746 (1997).
  19. S. Oda, T. Tanimura, T. Hoshida, C. Ohshima, H. Nakashima, Y. Aoki, L. Lei, Z. Tao, and J. C. Rasmussen, "Interplay between PMD and nonlinearity in 112 Gb/s DP-QPSK transmission with co-propagating 10.7 Gb/s NRZ channels," *Optical Fiber Communication Conference'11, OWO4*, (2011).
  20. D. Rafique, J. Zhao, and A. D. Ellis, "Compensation of nonlinear fibre impairments in coherent systems employing spectrally efficient modulation format," accepted for publication, *IEICE*, (2011).
- 

## 1. Introduction

The growing bandwidth demand from bandwidth-intense digital multimedia applications [1] continues to press the capacity requirement on the optical transmission systems. Increasing the transmission capacity requires increasing the spectral efficiency, and this has led to considerable research activity in advanced modulation formats employing coherent detection [2]. In particular, polarization multiplexed quadrature phase shifted keying (PM-QPSK) has been widely acknowledged as an optimum modulation format and has been investigated under various transmission scenarios [3,4].

Nevertheless, such an increase in transmission capacity emerges at the expense of increased susceptibility to linear and nonlinear fibre impairments, alongside more complex design architecture. With the availability of current digital signal processing (DSP) techniques and high-speed analog-to-digital converters (ADC) for 40- and 100 Gb/s systems, electronic mitigation of transmission impairments has emerged as a promising solution. As linear compensation methods have matured in the past few years [5,6], research has intensified on nonlinear impairments compensation [7–9]. In particular, electronic signal processing using digital back-propagation (DBP) with inverse fibre parameters or time inversion has been applied to the compensation of channel nonlinearities [9–13]. However, the complexity of DBP is currently exorbitant due to significantly high number of processing steps required in such calculations. In order to address these issues, simplifications in the DBP algorithm employing single-step per span or less via DBP techniques [11–15] have already commenced.

In this paper we investigate through numerical simulations, a simplified DBP algorithm based on the correlation of signal power in neighboring symbols when applying nonlinear phase compensation, and optimization of the position of nonlinear compensator, which requires less than one processing step per transmission span. We test the algorithm on a 112 Gb/s PM-QPSK system, in a 1,600 km (20x80km) transmission system, and show that a considerable complexity reduction can be achieved compared to standard DBP methods [11,14].

## 2. Theory

### 2.1 Digital back-propagation

Digital back-propagation processes the received signals by launching them into a virtual fibre with link parameters of opposite-sign values of those in the transmission channel. In practice, this method can be implemented by calculating the nonlinear Schrödinger equation (NLSE) governing the signal propagation through the fibre channel at the receiver. The NLSE governing the forward-propagation (for single-polarization) is written as [16]:

$$\frac{\partial E}{\partial z} + \frac{\alpha}{2} E + \underbrace{\frac{i\beta_2}{2} \frac{\partial^2 E}{\partial t^2} - \frac{\beta_3}{6} \frac{\partial^3 E}{\partial t^3}}_{LC} - \underbrace{i\gamma |E|^2 E}_{NLC} = 0 \quad (1)$$

where  $E$  is the envelope of the optical field,  $\beta_j$  represents the  $j^{\text{th}}$  coefficient of the Taylor series expansion of the propagation constant  $\beta$ ,  $\alpha$  is the fibre loss coefficient,  $\gamma$  is the nonlinear parameter,  $t$  is the retarded time. For back-propagation, Eq. (1) is numerically solved using the split step Fourier method (SSFM) [9], where  $\alpha$ ,  $\beta$  and  $\gamma$  are set to be the exact opposite values to those in the transmission fibre, and the optical amplifiers (power gain  $G$ ) are replaced with optical attenuators (power gain  $1/G$ ). The fibre is treated as a series of linear sections (where only  $LC$  is considered), and nonlinear sections (where only  $NLC$  is considered). In the absence of noise, back-propagation method can fully compensate the deterministic linear and nonlinear fibre impairments to arbitrary precision, provided that sufficient steps are taken in each fibre span. However, a compromise must be found between accuracy and complexity.

## 2.2 DBP simplification (weighted digital back-propagation)

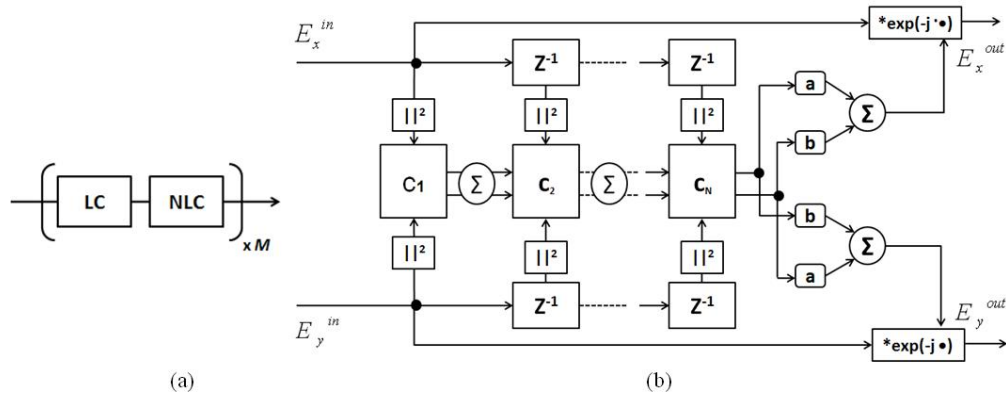


Fig. 1. (a) Schematic of digital back-propagation method, (b) Schematic of modified nonlinear compensation segment.

The principle of weighted DBP (WDBP) algorithm is to correlate the nonlinear shift at a specific symbol location with the power of various consecutive symbols, rather than only one, thus taking into account the phenomenon of dispersion induced power “spilling” into neighboring symbols. Indeed, this causes the power profile at each amplifier stage (i.e. when power is highest and most of the nonlinear shift takes place) to be the overlap of a larger number of dispersion-broadened pulses. Figure 1(a) shows the schematic of the WDBP method, similar in concept to the asymmetric SSFM [8] approximation to solve the NLSE, albeit with a much coarser step-size. The algorithm consists of a series of linear and nonlinear elements, where each LC is responsible for CD compensation using FFT/IFFT algorithms [17] and each NLC is responsible to compensate nonlinear phase shift imposed along a certain fibre section. Figure 1(b) shows the schematic of the modified nonlinear segment. The incoming digital data streams correspond to complex electric field vectors for  $x$  and  $y$  polarization states, and the correlation between neighboring symbols is taken into account by applying a time-domain filter corresponding to the weighted sum of neighboring symbols. Given a coarse step-size ( $>$  dispersion length), nonlinear phase shift (NLPS) on a given symbol is a weighted NLPS from adjacent symbols, as shown in Eq. (2a) and Eq. (2b),

$$E_x^{out} = E_x^{in} \times \exp \left[ -j \sum_{k=-(N-1)/2}^{(N-1)/2} c_k \left\{ a \left| E_x^{in} \left( t - k \frac{T_s}{2} \right) \right|^2 + b \left| E_y^{in} \left( t - k \frac{T_s}{2} \right) \right|^2 \right\} \right] \quad (2a)$$

$$E_y^{out} = E_y^{in} \times \exp \left[ -j \sum_{k=-(N-1)/2}^{(N-1)/2} c_k \left\{ a \left| E_y^{in} \left( t - k \frac{T_s}{2} \right) \right|^2 + b \left| E_x^{in} \left( t - k \frac{T_s}{2} \right) \right|^2 \right\} \right] \quad (2b)$$

where  $E_{x,y}^{out}$  and  $E_{x,y}^{in}$  are the electric fields for orthogonal polarization states before and after WDBP for  $x$  and  $y$  polarization states,  $a$  and  $b$  represent intra-polarization and inter-polarization parameters [11],  $N$  represents the number of symbols (or filter length) to be considered for a nonlinear phase shift,  $c_k$  is the weighing vector,  $k$  is the delay order, and  $T_s$  is the symbol period. Note that the values for  $a$  and  $b$  were found to be almost identical since we considered the Manakov model [18] for fibre propagation; and further details on optimization of these parameters can be found in [11,14]. It also is worth mentioning that the complexity reduction via WDBP is primarily achieved from the reduction in required FFTs rather than the reduced number of steps for NLC calculations.

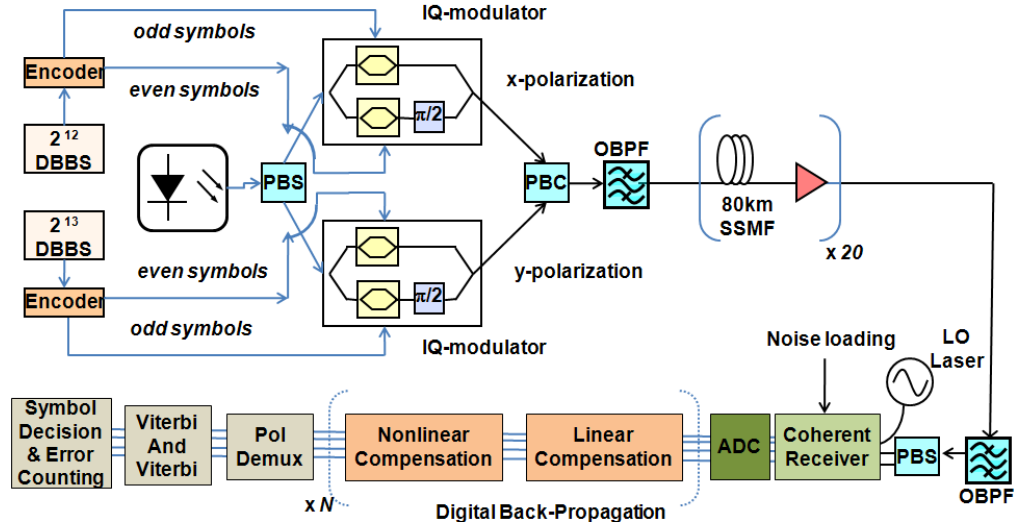


Fig. 2. Simulation setup for 112 Gb/s PM-QPSK with 20 spans employing digital back-propagation with  $N$  steps for the whole link. PBS: Polarization beam splitter, LO: Local oscillator, ADC: Analogue to digital converter.

### 3. Simulation setup

Figure 2 depicts the PM-QPSK transmitter setup at 112 Gb/s, the transmission link, and the receiver structure. The transmitter consists of a 1550nm laser with 500 kHz line-width, followed by a polarization beam splitter (PBS), and two nested Mach Zehnder modulators (one per polarization component), each driven by two 28 Gb/s bit sequences of length  $2^n$  which were properly pre-coded in order for the resulting QPSK optical signal to be phase-modulated by a De Bruijn binary sequence (DBBS,)  $B(4,n)$ , of order  $n$ . Different sequence orders ( $n = 13$ , and  $n = 12$  respectively) were used in order to obtain un-correlated data for each polarization component. Finally the two polarization components were combined by means of an ideal polarization beam combiner and the resulting 112 Gb/s PM-QPSK was passed through a 35 GHz 3<sup>rd</sup> order Gaussian filter and sent over the transmission link consisting of twenty spans comprising an erbium doped fibre amplifier (EDFA) followed by 80 km of standard single mode fibre (SSMF). The fibre had attenuation ( $\alpha$ ) of 0.2 dB/km, dispersion ( $D$ ) of 16 ps/nm/km, and a nonlinearity coefficient ( $\gamma$ ) of 1.5/W.km. The optical amplifiers were modeled as ideal noise-free EDFAs and white Gaussian noise was added at the receiver in order to calculate the OSNR required to obtain  $BER = 10^{-3}$  ( $OSNR_{req}$ ). Cross-polarization non-linear effects were included according to the Manakov model [18] and polarization mode dispersion (PMD) was neglected. Note that PMD may influence the

nonlinear system performance depending on the launch power and channel spacing of a given system, as shown in [19].

After fibre transmission, the received signal was pre-amplified (constant power of 0 dBm) filtered using a 35 GHz bandwidth 3rd order Gaussian optical band-pass filter. The optical signal was then coherently detected using a homodyne receiver, low pass filtered and down-sampled to 2 samples per symbol. Note that that increasing the oversampling ratio would increase the precision. However, we have recently demonstrated that for resolution greater than equal to 2 samples per symbol, the performance after DBP is almost constant [20]. The digital field was reconstructed using the inphase/quadrature components of each polarization and the signal was digitally processed. The transmission impairments were compensated using our WDBP algorithm explained in the previous section, where a series of  $LC + NLC$  steps was employed and the coefficients  $a, b$  and  $N$  were optimized. After the compensation of CD and non-linear phase shift, polarization demultiplexing was performed using a standard butterfly structure using four CMA adaptive filters with up to 7 taps each (the number of filter taps were optimized for each OSNR value) and the carrier phase was recovered using the Viterbi and Viterbi method. Finally the symbol decisions were made and errors were counted. All the numerical simulations were carried out using VPI@v.8.3, and digital post-processing was performed in Matlab@v.7.10.

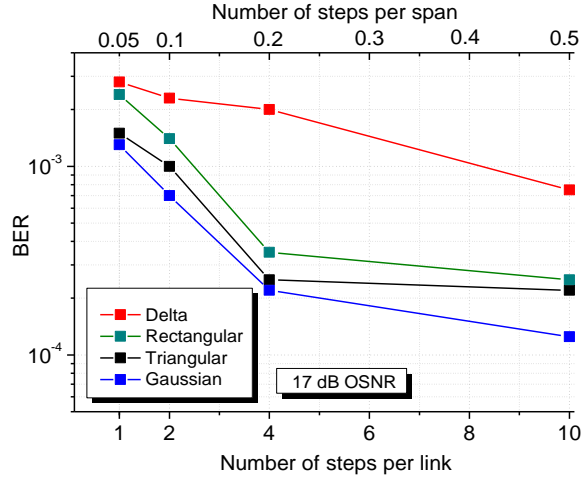


Fig. 3. BER as a function of number of WDBP steps per link with various filter shapes. Delta (circle), Rectangular (down triangle), Triangular (square), Gaussian (up triangle).

#### 4. Results and discussions

In order to establish the optimum time-domain filter profile (shape and filter coefficients) for WDBP algorithm, we employed various time-domain filters, and characterized the system performance by calculating BER as a function of number of WDBP steps, as shown in Fig. 3. The filter profiles for rectangular, triangular, and Gaussian shapes were given by,

$$rect(N) = \Pi\left(\frac{N - N_o}{2}\right), \quad tri(N) = \Lambda\left(\frac{N - N_o}{2}\right), \quad gauss(N) = e^{-\left(\frac{N - N_o}{2\sigma}\right)^2} \quad (3)$$

where  $\Pi$  and  $\Lambda$  represent rectangular and triangular functions respectively,  $N_o$  represents the filter offset,  $\sigma$  is a width parameter equal to the width of rectangular, half-width of triangular, and the standard deviation of the Gaussian distribution. In Eq. (3) we set the offset parameter  $N_o$  such that the first taps had a value of  $10^{-3}$  for Gaussian pulse and the first finite value for rectangular and triangular profiles. For each configuration we ascertained the minimum number of taps required to ensure that the decrease in BER for the next tap to be added was

less than 5% of the current BER. It can be seen from Fig. 3 that Gaussian approximation enables the lowest BER performance, and in this configuration the minimum required number of taps for the step-sizes of 1, 2, 4, and 10 were found to be 21, 17, 15 and 7, respectively. Note that the filter profile was always fixed to be Gaussian in the following analysis.

Figure 4(a) depicts the performance of the WDBP algorithm with varying precision (measured as total number of back-propagation steps). The results are plotted in terms of  $OSNR_{req}$  as a function of launch power ( $P_{in}$ ). In the absence of nonlinear compensation,  $OSNR_{req}$  degrades rapidly and above 4 dBm, BER of  $10^{-3}$  cannot be achieved due to strong intra-channel nonlinear effects at high launch powers. However, when WDBP is employed with only single step for the whole link, a significant improvement of about ~2.5 dB is observed, e.g. at 4 dBm. As the precision of WDBP is enhanced, one can see a gradual improvement in  $OSNR_{req}$ , e.g. ~4.5 dB  $OSNR_{req}$  improvement with respect to the case with no NLC can be observed with 20 steps at the  $P_{in}$  of 4 dBm. Nevertheless, there is still a visible penalty with respect to the back-to-back  $OSNR_{req}$ , due to the coarse step-size employed to keep the step-count minimal. We expect the performance to improve further given higher number of steps per span are employed, as it has been reported previously [10].

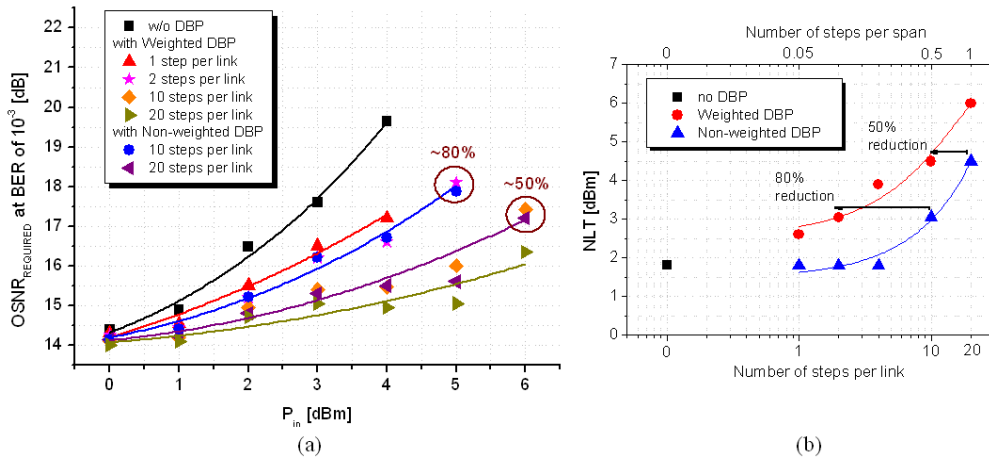


Fig. 4. (a) Required OSNR as a function of launch power after 20 spans. No DBP (squares), WDBP: 1 step (up triangles), 2 steps (stars), 10 steps (diamonds), NWDBP: 10 steps (circles), 1 step (left triangles), (b) Nonlinear threshold defined at 3dB  $OSNR_{req}$  penalty with respect to back-to-back case for various cases in Fig. 4(a). no DBP (square), WDBP (circles), NWDBP (triangles).

In order to compare our results with previously proposed DBP methods, we also employed recently proposed asymmetric SSFM based DBP [11], we will call it non-weighted DBP (NWDBP), which is based on instantaneous power dependent nonlinear phase shift and employs single step per span for DBP calculations. Comparing the two approaches, it can be observed that the  $OSNR_{req}$  with 10 steps for the whole link (NWDBP) is equivalent to that of WDBP algorithm with only 2 steps for the link. This shows a significant 80% reduction in required DBP steps with our new approach. Similarly, as we increase the number of step with WDBP method, the performance for 10 steps WDBP and 20 steps NWDBP almost converge, i.e. ~50% less step calculations. Note the decrease in the margin of complexity reduction as the number of steps is increased for WDBP method. This is due to the better precision for NWDBP when higher number of steps are employed, leaving less scope of improvement with WDBP, however one can still observe that 20 steps for the whole link with WDBP method still outperforms the NWDBP algorithm. This trend is also shown in Fig. 4(b) which shows the nonlinear threshold (NLT) – defined as the launch power for which the  $OSNR_{req}$  is increased by 2 dB compared to back-to-back – for all the cases in Fig. 4(a). Here one can clearly see that the nonlinear tolerance of WDBP is significantly better than traditional DBP method and one can employ as few as 2 steps for the whole link. It is worth mentioning that

complexity reductions (reduced number of required DBP steps) in proportion to the ones reported here, have been recently proposed using a back-propagation technique employing an analogous frequency-domain filtering approach [12], which further validates our results.

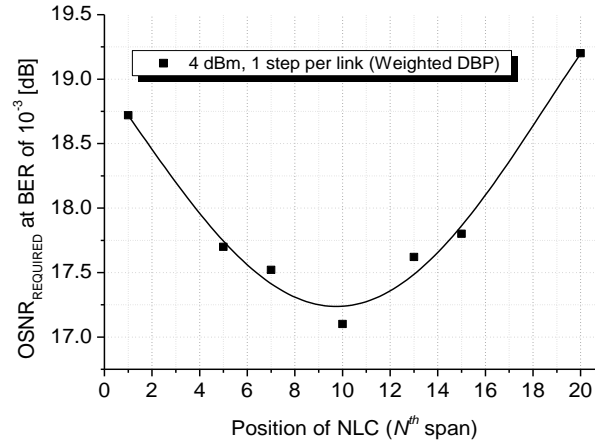


Fig. 5. Required OSNR as a function of position of NLC, with single step for the whole link (20 spans) at a launch power of 4 dBm.

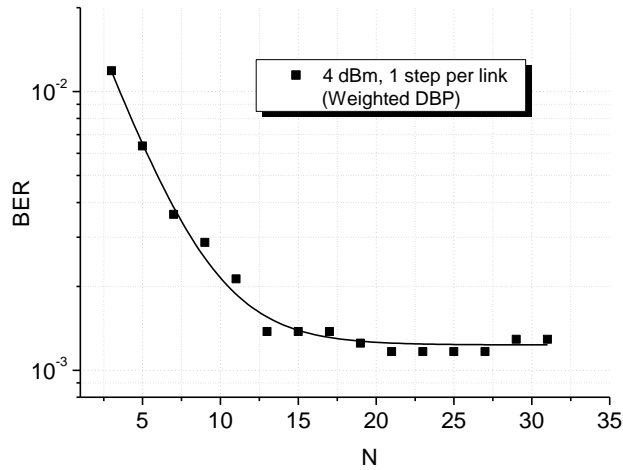


Fig. 6. Filter length as function of BER, with single step for the whole link (20 spans) at a launch power of 4 dBm.

Figure 5 and Fig. 6 show the two degrees of freedom we exploited to reduce DBP steps, i.e. the position where NLPS is applied for a given fibre segment, or the position of NLC compensator, and the length of filter window we used to take advantage of the correlation between symbols, respectively. Figure 5 illustrates the position of NLC when the whole link is compensated with only 1 step. It can be seen that when multiple fibre sections are compensated using a single step, the optimum position of NLC is found to be in the middle of the link, or after the 10th span in this case. We attribute this trend to the fact that given symmetric position is used for NLC, the nonlinear phase shift is not overcompensated for subsequent steps (we applied a symmetric positioning rule for higher number of steps with WDBP method, and verified it across a range of step-size choices. For e.g., optimum positions for NLC were found to be after the 7th and the 14th span, if 2 steps per 20 span link were employed). Figure 6 depicts the length of averaging filter which was used to apply the nonlinear phase shift with single step for the whole link. It can be seen that the window of

about 21 symbols is enough to get the optimum performance. Note that this is the maximum window we employed for this method, since with 1 step for the whole link, the uncompensated signal is dispersed at most, compared to higher number of steps; which again emphasizes the efficiency of WDBP method.

## **5. Conclusions**

We have shown that the required number of digital back-propagation steps can be reduced significantly by considering the correlation between adjacent symbols, and by optimizing the position of nonlinear compensator segment. We report a significant reduction in required back-propagation steps, up to 80% compared to the previously proposed conventional DBP methods. Furthermore, we report that when multiple fibre spans are compensated using a single back-propagation step, mid-step placement of nonlinear compensator gives the optimum result. We have also investigated different correlation filter shapes and lengths and found that the Gaussian approximation gives optimum results with a maximum filter length of 21 symbols for one step per link. In view of near future optical network deployments we believe that this approach will make nonlinear compensation practically viable, given the radical complexity reductions that have been reported.

## **Acknowledgments**

The work described in this paper was carried out with the support of the EUROFOS project, Network of Excellence funded by the European Commission through the 7th ICT-Framework Programme; Science Foundation Ireland under Grant 06/IN/I969p; the Italian Ministry of University and Research project PRIN 2008MPSSNX, the Italian Ministry of Foreign Affairs (Direzione Generale per la Promozione e la Cooperazione Culturale) and the agreement with ISCTI, Rome, Italy.